Band structure, optical properties and infrared spectrum of glycine–sodium nitrate crystal

J. Hernández-Paredes, Glossman-Mitnik, H.E. Esparza-Ponce, M.E. Alvarez-Ramos, A-Duarte-Moller

Abstract

Glycine–sodium nitrate, GSN, crystals were grown from a stoichiometric solution by slow cooling technique and were characterized by optical absorption and FTIR spectroscopy. The data collected by FTIR were compared with the vibrational spectrum theoretically obtained by using DMol code in the local density approximation LDA. Moreover, the crystal band structure, the density of states, and the optical absorption data were calculated by using the CASTEP code within the framework of LDA and the generalized gradient approximation GGA. The calculations are in good agreement with the structure and properties of GSN; e.g., the optical transparency in visible region, the low density, the insulate character, and the bipolar form of glycine molecule.

Introduction

The research field of non-linear optics (NLO) investigates new materials that can be used to build optical devices like frequency doublers and optical modulators. Recent investigations focus on the design of new materials that attain second order optical processes, as well as the strong interaction with the oscillating electric field of light. Materials based in a mixture of amino acids with ionic salts have been investigated in the NLO field and have been recognized as materials that have good nonlinear optical properties [1–3].

GSN has proven to have characteristics showing to be a candidate for nonlinear optic applications. Single crystals of GSN were grown by Narayan Bhat and were reported as having greater efficiency in second harmonic generation (SHG) than potassium dihydrogen phosphate (KDP) [4]. GSN has a non-centrosymmetric crystalline structure formed by alternating layers of sodium nitrate and glycine molecules throughout the (001) direction.

Ab-initio calculations have gained recognition in recent years, because they have shown to be important when predicting the properties of the new materials. Furthermore, optical measurements in crystals require a specialized laboratory, as well as excellent quality materials, which is generally expensive. DFT is an alternative for predicting optical properties with good agreement. For these reasons, some molecular crystals similar to GSN have been investigated with DFT to calculate their optical and electronic properties, such as diglycine nitrate (DGN) [5] and tryglicine sulphate (TGS) [6]. In both investigations the calculations describe the characteristics of materials with enough accuracy.

Nevertheless, theoretical calculations based on DFT have not been made to determine the electronic and optical properties of GSN. This tool offers the capability to study materials with a simple and inexpensive scheme. Therefore, in the present work we report for the first time the electronic and optical properties of GSN obtained by computational simulation. The absorption and infrared spectrums are in agreement with the experimental results. Furthermore, DFT calculations depict the characteristics of the material, which are related to the molecular character and crystalline structure.

Methods and computational details

Experimental details

Seeds of GSN were grown in a few weeks by the slow evaporation technique at a constant temperature of 30°c from a saturated solution. The solution was prepared by mixing an equimolar ratio of glycine (NH_2CH_2COOH) JT-Baker 98.8% pure with sodium nitrate ($NaNO_3$) JTBaker with a purity of 99.99% and by dissolving them in 100 mL of double-distilled water. The solution was stirred continuously for an hour to get a saturated solution. Then it was filtered and transferred to a precipitation vessel covered with a perforated cap to prevent impurities.

The synthesized salt was then purified by repeated crystallization. Transparent GSN seeds were formed by spontaneous nucleation, in which the higher quality ones were selected because of their transparency and lack of macrodefects. These seeds were added to a saturated solution of GSN to high temperature, and this solution was placed in a growth crystallizer. GSN crystals were grown with temperature lowering of 1°c/day at range of 40-22°C.

A possible reaction mechanism of the chemical synthesis is as follows:

$NH_2CH_c\text{-}COOH+NaNO_3 \rightarrow NH_3CH_2COO{\cdot}NaNO_3$.

Functional groups present in the crystals were found using Fourier transform infrared spectroscopy (FTIR). The IR analysis was recorded at room temperature with a Nicolet Magna IR 7500 spectrometer, within wave number range of 400–4000 cm^{-1}. Crystals of GSN were finely ground and mixed with powdered KBr. The mixture was pressed to obtain a transparent disc in order to take the IR spectrum. The optical transparency of crystals was measured by UV–visible spectroscopy. The UV–visible characterization of

GSN crystals was recorded with a lambda 10 Perkin Elmer UV–VIS spectrometer in the range of 1100–200 nm over a sample with a crystal thickness of 2.5 mm.

Computational details

All calculations were performed using Materials Studio 3.2 software [7] within the framework of the density functional theory DFT. The infrared spectrum was calculated with Dmol [8] module. A DNP (Double Numerical extra polarization) basis set [9,10] was used which includes polarization polarization functions. In order to calculate the energy, band structure, density of states, and optical absorption spectra a module CASTEP (Cambridge Total Serial Energy Package) was employed [11] by the local density approximation method (LDA) of Ceperly and Adler [12] parameterized by Perdew and Zunger [13] and the CA–PZ functional, in addition to a generalized gradient approximations (GGA) in the scheme of Perdew, Burke, and Erzerhof (PBE) [14] for the interchange and correlation effects was employed. Norm-conserving pseudopotentials were employed in order to obtain optical properties. In order to confirm the convergence of calculations, the calculations were optimized with respect to the cutoff of energy required in calculations of solid state with the scheme of Lin et al. [15]. Total energy dependence on the energy cutoff (Ecut) was of 770.0 eV that corresponds to a criterion of convergence of 0.1×10^{-5} eV/atom. In both cases optical properties were calculated with 250 k points in the Brillouin zone. The atomic coordinates of the GSN crystal were obtained from the Cambridge Crystallographic Data Centre [16].

Results and discussion

IR spectra

Theoretical and experimental IR spectra are shown in Fig. 1. All the features observed in the experimental IR spectrum have been assigned by comparison with DFT calculations. Amino acids usually exist as zwitterions in crystals. They have an ionized carboxyl group (COO^-) and an amine salt NH_3^+.

In the experimental spectrum of GSN, NH_3^+, stretching mode bands were found with broad band strength and multiple peaks between 3100 and 2600 cm^{-1}. This same mode could be seen at low frequencies up to 2200 cm^{-1}. At a 2036 cm^{-1} frequency, a primary amine resonant frequency was found and was produced by a combination band of NH_3^+ asymmetric deformation and NH_3^+ rotation. A band of 1654 cm^{-1} corresponded to NH_3^+ deformation and a 1511 cm^{-1} corresponded to symmetric deformation. In theoretical spectrum principal bands are matched to: 3200 and 2247 cm^{-1} for NH_3^+ stretching mode and 1707 cm^{-1} for NH_3^+ deformation.

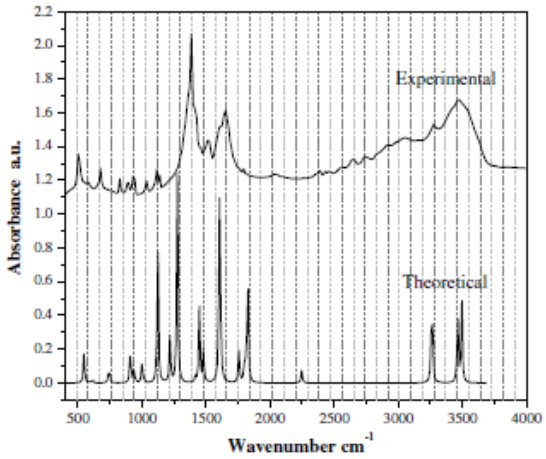

Fig. 1. IR spectra of GSN.

Two overlapped bands at 1613 and 1411 cm^{-1} were attributed to the asymmetric and symmetric stretch modes of the COO^- group. These are matched with 1607 and

1447 cm^{-1} in theoretical spectrum. Other bands of COO^- mode deformation were shown at 676, and at 503cm^{-1} in experimental spectrum. In the theoretical spectrum, these peaks corresponded to 617 and 503 cm-1. Both results confirmed that the glycine molecule existed in a zwitterion form inside the crystal. This caused an antiparallel arrangement, which contributed to non-centrosymmetric crystalline growth. The strongest absorption at 1396cm^{-1} was due to asymmetric NO_3 stretch and also appeared at 927 cm^{-1} as a weak band. More variable bands were found matching amino acids.

The theoretical IR spectrum was calculated in gas phase for a single GSN molecule. Differences between experimental and theoretical spectrums are attributed mainly to atomic interactions occurring in the solid phase. Table 1 presents the experimental and the calculated vibrational frequencies for GSN.

Electronic and optical properties

GSN exhibits a monoclinic non-centrosymmetric crystalline structure with space group *Cc*. Its lattice parameters are *a* = 14.329 (3) Å, *b*= 5.2662 (11) Å, *c*= 9.1129 (18) Å, and β = 119.10 (3) ° [17]. The unit consists of one glycine molecule and one sodium cation and one nitrate anion. The glycine molecules are flanked by layers of $NaNO_3$. Fig. 2 shows the crystal structure of GSN.

Table 1
Experimental and theoretical comparison of selected IR bands

Assignment	Experimental (cm^{-1})	Theoretical ($Dmol\,cm^{-1}$)
NH_3^+ stretching	3100–2600	3200
NH_3^+ asymmetric deformation	2036	–
NH_3^+ asymmetric deformation	1654	1707
COO^- asymmetric stretch	1613	1607
NH_3^+ symmetric deformation	1511	1480
COO^- symmetric stretch	1411	1447
NO_3 asymmetric stretch	1386	1277
N–N rocking	1139	1140
N–N rocking	1116	1127
NO_3	1035	1007
CH_2 rocking	931	937
C–C stretching	896	901
NO_3 asymmetric stretch	827	739
COO^-	676	617
COO^- deformation	584	595
COO^- deformation	503	503

The Brillouin zone that corresponds to the monoclinic structure is shown in Fig. 3. The directions with greater symmetry which were used to calculate the electronic properties are marked with special points.

The calculated band structure for GSN in LDA frame is shown in Fig. 4 and for GGA in Fig. 5. The results accurately described the electronic properties of GSN. The states below the Fermi level were quite flat, so the dispersion was about 0.5 eV. The excited states above 4.5 eV were slightly altered by the crystalline field and correspond to glycine states. Minimum dispersion occurs along $Y \rightarrow A$ and $E \rightarrow C$ directions that belong to larger crystallographic axis *a* because of the separation between layers of glycine and sodium nitrate are linked by coordination bonds involving the Na atom and the O of the carboxylate ions whose values are on the order of 2.410 Å.

In the first two excited states, a slight dispersion of about 0.5 eV is observed for both calculations, but bands with greater dispersion of approximately 1.3 eV appear in the followed excited states and these corresponds to the parallel directions of the B* axis.

The directions are: G → Y, A → B, and D → E. These directions display a greater atomic density than the others. Therefore, the influence of the crystalline field is reflected in the dispersion value, which contributes to the energy dispersion of the bands. Besides, a stronger contribution is due to presence of coordination bonds between glycine molecules. These molecules are clearly aligned and do not display discontinuities throughout the parallel B* and C* axes.

GGA band structure showed less dispersion than LDA. This is expected because, the overbinding of atoms characteristic of the LDA functionals is generally

corrected when using GGA functionals. Both calculations are in agreement with the similar crystal of DGN reported by Andriyevsky [6]. The magnitudes of the wave vector dispersion can be attributed to a relatively large molecular distances of GSN. These distances cause the low density of GSN crystal 1.76 g/cm^3.

Smaller gap than can be experimentally obtained is expected for DFT calculations which generally underestimate the band gaps of insulators and semiconductors. The gap is directly at symmetry point G, the valence and conduction bands correspond to a bonding and antibonding states of NO_3. Its value is 2.98 eV for LDA calculations which is in close agreement with the 2.99 eV obtained by the GGA, although this value is not clearly observed in the absorption spectrum obtained experimentally. Nevertheless, the energy between the ground and the exited states of glycine groups is accordance with the maximum band absorption shown experimentally at 4.15 eV and is clearly observed in density of states (DOS) representation illustrated in Figs. 6 and 7 for LDA and GGA calculations, respectively.

The DOS plot was produced with a smearing width of 0.2 eV, with the Fermi level E_F arbitrarily placed at 0 eV.

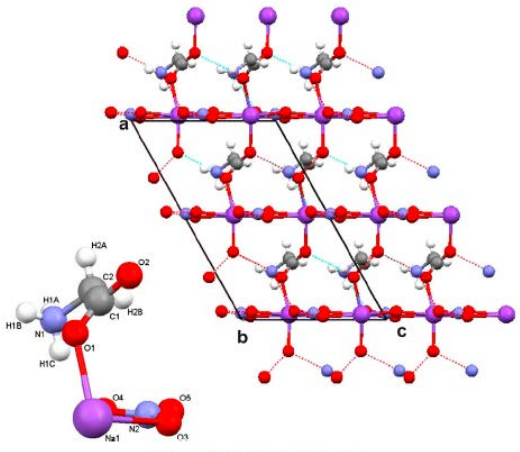

Fig. 2. GSN crystal shown in the *ac* plane.

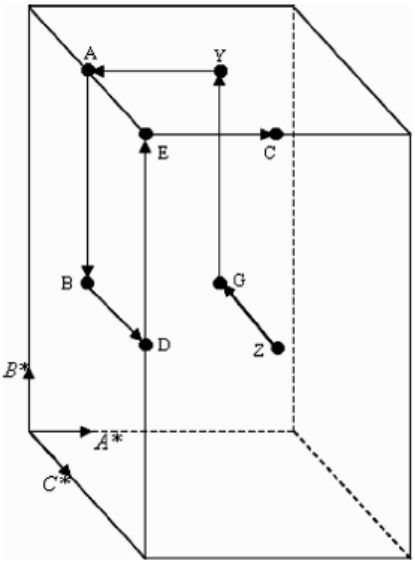

Fig. 3. Brillouin zone of GSN crystal.

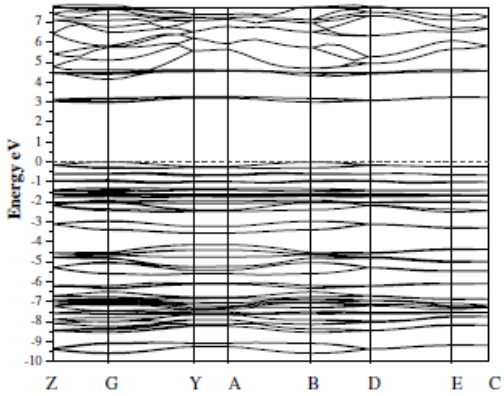

Fig. 4. Calculated band structure of GSN crystal with LDA at 295 K: Z—[0, 0, 1/2], G—[0, 0, 0], Y—[0, 1/2, 0], A—[−1/2, 1/2, 0], B—[−1/2, 0, 0], D—[−1/2, 0, 1/2], E—[−1/2, 1/2, 1/2], C—[0, 1/2, 1/2].

The results of the density of states showed the distribution of *s* and *p* electrons in the energy bands. The overall distributions of states across the energy range of DOS are similar to that of DGN and TGS molecular crystals. In both calculations it is observed that the conduction band above the Fermi level is occupied approximately 98% by *p* type electrons associated mainly with the NO_3 anion. The following

unoccupied states are principally due to carboxylate or guanadyl states of glycine molecule and are formed by a mixture of s and p characters. LDA gives an occupation of about 65% for p states and 71% for GGA. These states are consistent with the absorption edges the UV–vis spectra.

The *p* character in the narrow valence band just below the Fermi level is 98% and decreases to about 73% for the occupied states in the range of -3 to -10 eV and continued to reduce until 42% for the states below to .10 eV when they were mainly s states. As expected for molecular crystals, glycine and NO_3 groups create quasi-separated states.

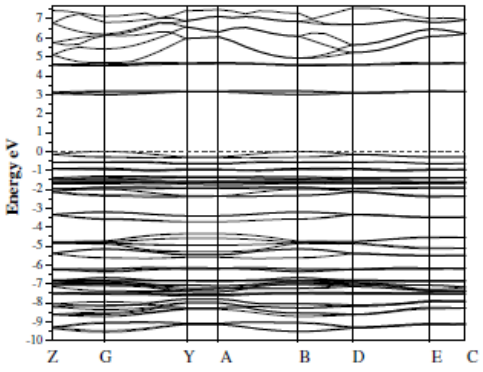

Fig. 5. Calculated band structure of GSN crystal with GGA at 295 K: Z—[0, 0, 1/2], G—[0, 0, 0], Y—[0, 1/2, 0], A—[−1/2, 1/2, 0], B—[−1/2, 0, 0], D—[−1/2, 0, 1/2], E—[−1/2, 1/2, 1/2], C—[0, 1/2, 1/2].

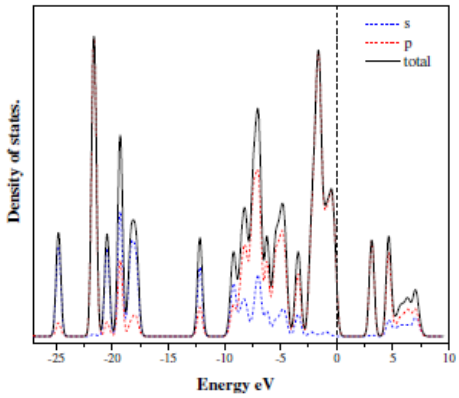

Fig. 7. Calculated DOS for GSN GGA.

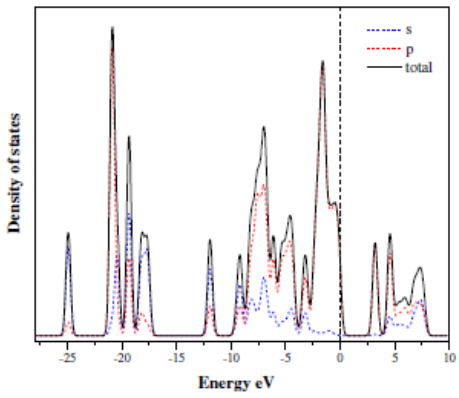

Fig. 6. Calculated DOS for GSN LDA.

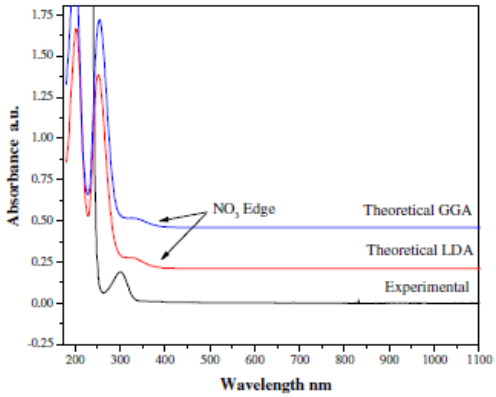

Fig. 8. Experimental and theoretical absorption spectra.

We performed a simulation of the absorption spectra for the GSN crystal in the polycrystalline sample and compared the calculations obtained experimentally. The corresponding results are presented in Fig. 8 where one can clearly see that the maximums values of absorbance matched the ones obtained experimentally. However, both calculated spectrums showed a slight edge that begins at about 400 nm, which is difficult to observe in the experimental spectrum because it is overlapped with the strong absorption in 300 nm and both states are observed as a pronounced single edge, attributable to a deviation in experimental measurement. Then, the theoretical results allow two separate states in the range to 400–250 nm, the first due to NO_3 antibonding state and is consistent with the band structure gap. The second was due to glycine and NO_3 states. Other noticeable characteristic in the absorption spectrums is a wide transparency window within the range of 400–1100 nm which is desirable for NLO crystals because the absorptions in an NLO material near the fundamental or second harmonic signals will lead to the loss of the conversion of SHG. Due to this property, GSN has potential uses for SHG using a Nd:YAG laser (1064 nm) to emit a second harmonic signal within the green region (532 nm) of the electromagnetic spectrum. But GSN is not a candidate for the third (355 nm) or fourth (266 nm) harmonics of Nd:YAG.

Fig. 9 shows the absorption spectra of GSN extended to 10 eV. The absorptions that the material presented after 5.5 eV, are mostly of the *p* type glycine and less of sodium nitrate.

The n_Y refractive index was calculated with LDA and GGA. In monoclinic structures the *Y* dielectric axis is taken parallel to the twofold crystallographic axis. In GSN crystal this axis matched with the *b* crystallographic axis. The other two dielectric

axes lie in the *ac* plane perpendicular to *b* axis and correspond to the highest and the lowest refractive indexes. In the case of GSN crystal, no experimental results of the refractive indices are found in the literature and nor the position of the other two dielectric axes. For this reason we only calculated n_Y. Thus, it is the middle index ellipsoid. It can be observed in Fig. 10 that the calculations of the refractive index with LDA are 5.9% greater than the calculated ones with GGA.

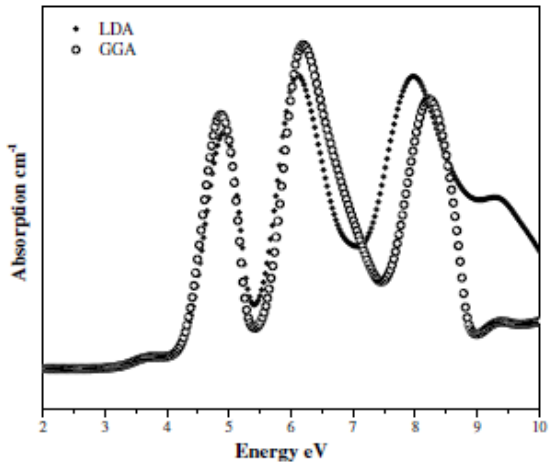

Fig. 9. Absorption spectra for GSN obtained for LDA and GGA.

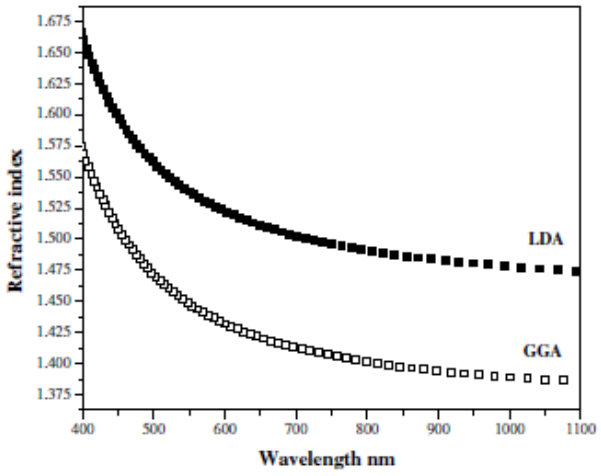

Fig. 10. n_Y Refractive index.

NLO studies

The SHG signal of GSN was measured by the powder technique of Kurtz and Perry [18]. The crystal was ground into powder and densely packed between two transparent glass slides. The second harmonic output was generated by irradiating powder samples by a pulsed-laser beam.

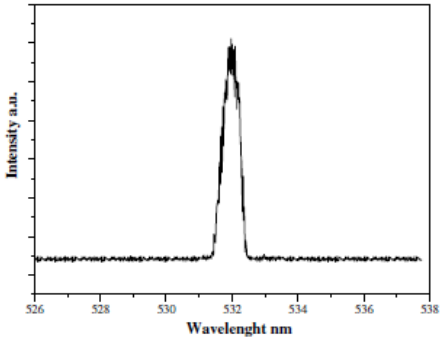

Fig. 11. 532 nm Emission spectrum of the GSN detected.

The source is Nd:YAG Quanta ray INDI series laser emitting 1064 nm, generating an 8 ns pulse and it was operated at 6 mJ/pulse and a repetition rate of 10 Hz. The second harmonic signal was analyzed with a Jobin–Yvon monochromator Triax320 and detected with a Hamamatsu R928 photomultiplier tube. Then, EGG/PAR 165 boxcar averager and readout processed it on a strip-chart recorder. The Fig. 11 shows the preliminary result of signal SHG experiment when the emission spectrum shows a strong signal around the 532 nm, wavelength corresponding to the half of 1064 nm used with the Nd–YAG laser beam. This measurement establishes that the frequency doubling has been obtained.

Conclusions

GSN crystals were grown by slow cooling technique. DFT calculations were in accordance with GSN characteristics and suggested its molecular character. The theoretical results of the IR spectra are close to those experimental ones and confirmed

the bipolar character of the glycine molecule in the crystal. Differences were due to the theoretical spectrum obtained for a single molecule of GSN, therefore the interactions with other GSN molecules were not considered. The electronic band structure was in accordance with the absorption spectrums and predicts that GSN is a semiconductor with a direct band gap of 2.9 eV. UV–vis spectra showed that GSN was optically transparent through 1100–350 nm and hence suitable for SHG. The first experimentally estimated optical absorption maximum was found to start at about at 300 nm. Nevertheless, a weak absorption at 400 nm corresponding to NO_3 groups and is noticeable by DFT. Absorption bands after 250 nm are principally due to glycine states. The n_Y refractive index calculated with LDA differs 5.9% from the calculated with GGA due to the overbinding of atoms characteristic of the LDA functionals. The SHG measurement establishes that the frequency doubling has been obtained.

Acknowledgements

The authors thank Roal Torres, Daniel Lardizaval, Enrique Torres, Armando Reyes, Luis de la Torre, and Wilbert Antunez (Centro de Investigacion en Materiales Avanzados S.C.) for their technical support. J. Hernandez- Paredes gratefully acknowledges a doctoral fellowship provided by CONACYT (National Council of Science and Technology in México).

References

[1] Katsuyuki Auki, Kozo Pagano, Yoichi Iitaka, Acta Crystallogr. B 27 (1971) 11.

[2] C. Razzetti, M. Ardoino, L. Zanotti, M. Zha, C. Paorici, Cryst. Res. Technol. 37 (2002) 456.

https://cimav.repositorioinstitucional.mx/jspui/

[3] M.D. Aggarwal, J. Stephens, A.K. Batra, R.B. Lal, J. Optoelectron. Adv. Mater. 5 (2003) 555.

[4] N. Narayan Bhat, S.M. Dharmaprakash, J. Cryst. Growth 235 (2002) 511.

[5] B. Andriyevsky et al., Physica B 364 (2005) 78–84.

[6] B. Andriyevsky et al., Physica B 373 (2006) 328–333.

[7] Materials Studio version 3.2, Accelrys Inc. San Diego, 2001.

[8] DMol3, Materials Studio 2.0, Accelrys Inc., San Diego, CA, USA

[9] B. Delley, J. Chem. Phys. 92 (1990) 508.

[10] B. Delley, J. Phys. Chem. 100 (1996) 6107.

[11] V. Milman, B. Winkler, J.A. White, C.J. Pickard, M.C. Payne, E.V. Akhmatskaya, R.H. Nobes, Int. J. Quant. Chem. 77 (2000) 895.

[12] D.M. Ceperley, B.J. Alder, Phys. Rev. Lett. 45 (1980) 566.

[13] J.P. Perdew, A. Zunger, Phys. Rev. B 23 (1981) 5048.

[14] J.P. Perdew, K. Burke, W. Ernzerhof, Phys. Rev. Lett. 77 (1996) 3865.

[15] J.S. Lin, A. Qteish, M.C. Payne, V. Heine, Phys. Rev. B 47 (1993) 4174–4180.

[16] CCDC No. 174799.

[17] R.V. Krishnakumar, M. Subha Nandhini, S. Natarajan, K. Sivakumar, Babu Varghese, Acta Crystallagr. C57 (2001) 1149.

[18] S.K. Kurtz, T.T. Perry, J. Appl. Phys. 39 (1968) 3798.